JJEE

Volume 12 | Number 1 | March 2026 | Pages 19-31

Jordan Journal of Electrical Engineering

ISSN (print): 2409-9600, ISSN (online): 2409-9619

Homepage: jjee.ttu.edu.jo

A New Modelling of Ferrite Core-based Receiving Coil in Wireless Power Transfer for Implantable Medical Devices

Ihab Anis Zergua[1], Naamane Mohdeb[2*], Nabil Ikhlef[3], Hicham Allag[4]

[1, 2, 3, 4] L2EI Laboratory, Department of Electrical Engineering, Jijel University, Algeria
E-mail: mohdeb.naamane@gmail.com

Received: Oct 25, 2025 *Revised: Jan 02, 2026* *Accepted: Jan 11, 2026* *Available online: Mar 19, 2026*

***Abstract*—** This paper focuses the use of ferrite rods to miniaturize the receivers used for inductive wireless power transfer. The aim of this work is to propose an implanted solenoid coil to wirelessly power capsules using inductive coupling. The diameter and thickness of the flexible transmitter coils are 42.2 mm and 1.2 mm, respectively. The diameter of the miniaturized RX is 1.5 mm and 10 mm-length, which is appropriate for integration within current commercially available capsules. In this work, the demagnetizing factors of a ferrite-core receiver are considered. At c = 26 mm, the power received is 14 W, which corresponds to a power transfer efficiency of 60 %. Nevertheless, the receiver was still able to draw a power of 6 W at 89% efficiency at a height of 10 mm, and 6 W at 13% efficiency at 50 mm. Considering the above, we have chosen to operate the WPT link for this work at 0.125 MHz. The proposed system represents a practical proposition for WPT in capsule endoscopy. The results indicate that it shows better performance in power transfer efficiency and power received, which is in good agreement with the experimental and simulation analysis.

***Keywords*—** Wireless power transfer; Demagnetization; Energy efficiency; Equivalent circuits; Ferrites; Magnetic resonance; Mutual coupling.

1. INTRODUCTION

In the last few decades, thanks to the technological advancement in electronics and micro and nanofabrication, wireless power transfer (WPT) systems have been very successful in different applications [1, 2]. WPT systems have become increasingly suitable solutions for the electrical powering of advanced multifunctional micro-electronic devices such as those found in current biomedical implants. The WPT technology provides reliable and convenient power charging for implant medical devices without additional surgery. The WPT devices are used to power implantable devices such as pacemakers, defibrillators, and neuro-stimulators. In order to implement these devices successfully, the WPT technology is often utilized because it provides an alternative to the battery as the energy source; reduces the size of implant substantially; allows the implant to be placed in a restricted space within the body; reduces both medical cost and chances of complications; and eliminates repeated surgeries for battery replacements [3]. This eliminates the need for frequent surgeries to replace batteries, improving patient comfort and safety [4].

The medical implants are often designed in a cylindrical or capsular shape such as the Bion® microstimulator [5]. For these cases, the use of a solenoidal coil is more common, see Fig. 1. Many papers focus on using ferrite receivers in applications with strict size/weight restrictions, such as biomedical devices. For example, Theilmann and Asbeck [6] developed extensive models and explored both theoretically and experimentally ferrite-core receivers with

* Corresponding author
DOI: https://doi.org/10.5455/jjee.204-1761424698

volumes appropriate for use in biomedical implants. High permeability materials, such as ferrite cores, are utilized to enhance the magnetic coupling [6-8]. For the WPT system with helix coils, a cylindrical ferrite core positioned in the receiving coil should improve the mutual inductance between coils. The receiver size is usually in the range from mm to several cm, and penetration depths are in the range from mm to several cm. Over 100 mW can be transferred at over 50% PTE, see Fig. 2 [9-11]. Some misalignment is tolerated, usually limited to roughly the largest coil radius. In [12], the distance between the transmitter and receiver is expected to be between 8 and 15 mm, and the radial misalignment is expected to be less than 15 mm. Higher frequencies are associated with smaller coils, which is advantageous in this case [12-14]. However, with increasing frequency, the losses in the coil also increase. A frequency of 0.125 MHz was chosen because the ferrite core in our device becomes lossy at frequencies of > 1 MHz. It was shown that at 5 MHz, 1 W can be transferred safely to a brain implanted visual prosthesis.

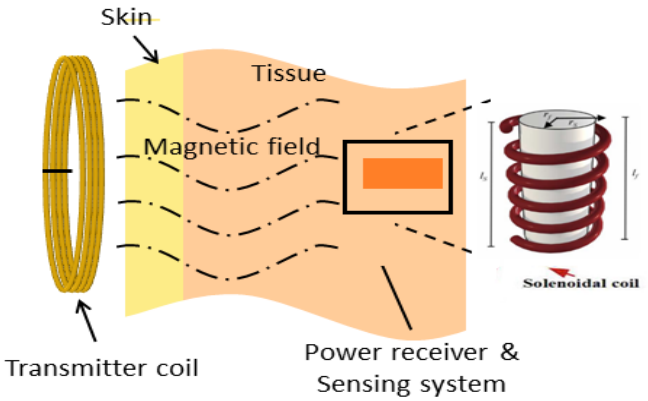

Fig. 1. The implanted solenoid coil.

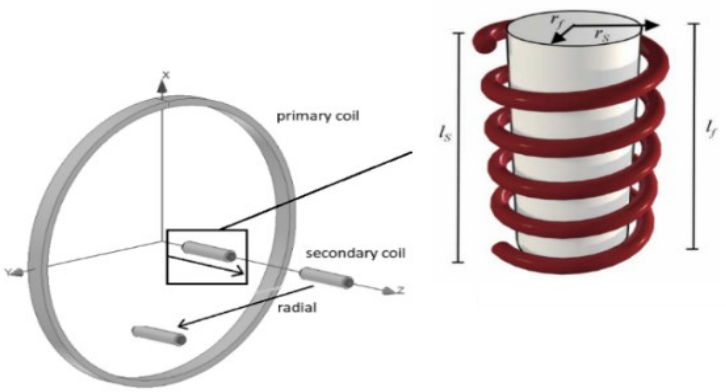

Fig. 2. Coil configuration for power transfer.

Several devices have been designed which utilize ferrite rods, but up to this point analysis of the performance enhancement provided by the ferromagnetic material has not been accurately reported. When designing implants authors often rely on their own experimental data to optimize device performance [6]. Other times a simplified understanding of the effect of ferrite cores is described, where it is stated that mutual inductance is increased by the relative permeability of the ferrite core with no mention of rod shape [15-17].

This research significantly advances the design of biomedical WPT systems by providing a high-accuracy analytical framework for deep-seated implants with variable orientations. By introducing a Fill Factor-adjusted mutual inductance model (M_{core}= M*FF), this work enables the miniaturization of ultra-lightweight receivers without sacrificing power efficiency.

Furthermore, the proposed equivalent coil method achieves a drastic reduction in 3D simulation complexity, allowing for rapid, real-time optimization of magnetic coupling in dynamic anatomical environments.

In this paper, a WPT system with a magnetic resonant structure is proposed to increase the magnetic field through the receiving coil. In Section II, the equivalent circuit model of the WPT system is presented, and the power transfer efficiency is calculated. The demagnetizing factor of the ferrite core is investigated; the analytical expressions of the mutual inductance for coils with cylindrical ferrite core, as well as the novel magnetic resonant structure, are explored. Simulation and experiments, compared in Sections 3, respectively, are conducted to validate the performance of the WPT system with coils with cylindrical ferrite core of the receiving structure. Finally, concluding remarks are drawn in Section 4.

2. WPT SYSTEM AND FORMULATION

In order to estimate the power transfer capability of the WPT system, a simplified inductive powering circuit is built (Fig. 3). In this model, the load of the implanted electronics to which power is delivered is represented by R_L. The rectifier is modeled with a diode D_1 and C_L . Analysis of this model is not trivial due to the nonlinearity of the rectifier. Therefore, we can converted it into a linear model by transfer the DC load into an AC equivalent linear load, as shown in Fig. 3.

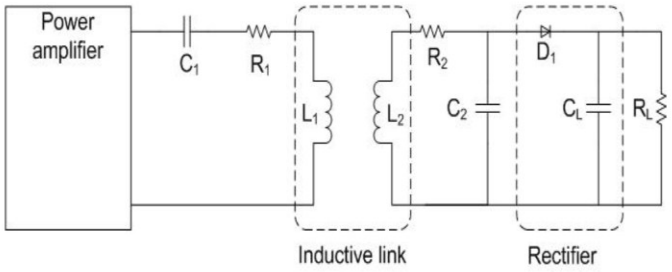

Fig. 3. System overview of an inductive power link for biomedical applications.

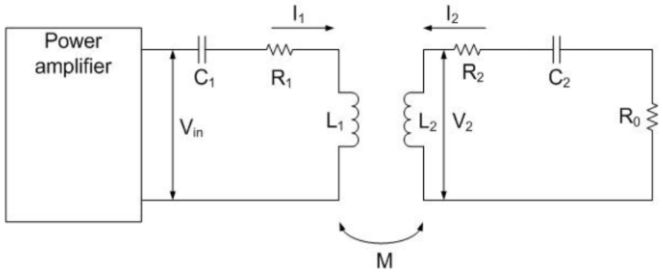

Fig. 4. The secondary stage is simplified with an approximated linear model.

With current direction defined as in Fig. 4, the voltage drop across each terminal can be express as the following equations because of the magnetic coupling effect between two coils [18]:

$$V_{in} = I_1\left(R_1 + j\omega L_1 + \frac{1}{j\omega C_1}\right) + j\omega\, MI_2 \quad (1)$$

$$V_2 = I_2 j\omega L_2 + j\omega\, MI_1 = I_2 j\omega(R_2 + R_0 + \frac{1}{j\omega C_2}) \quad (2)$$

Where V_{in} is the AC output voltage from the power amplifier, Vin and V_2 is the AC voltage across the secondary coil. M is the mutual inductance, associated with L_1 and L_2 by coupling coefficient, and is defined as [19]:

$$M = k\sqrt{L_1 L_2} \quad (3)$$

The relationship between the currents of receiver and transmitter coils can be derived as the following equation:

$$I_2 = I_1 \frac{j\omega_0 M}{R_2+R_0} \quad (4)$$

The total power transfer efficiency of the inductive link, defined as the ratio between the power delivered to the load and the output power from the power amplifier, is expressed as [20, 21]:

$$\eta = \frac{P_{out}}{P_{in}} = \frac{(\omega_0 M)^2 R_0}{(R_2+R_L)(R_1(R_2+R_0)+(\omega_0 M)^2)} \quad (5)$$

Through calculations, the received power of load can be expressed as:

$$P_{out} = \frac{{V_{in}}^2(\omega_0 M)^2 R_0}{(R_1(R_2+R_0)+(\omega_0 M)^2)^2} \quad (6)$$

The optimum efficiency is obtained introducing $R_{L,opt}$ given by Eq. (6). For the SS topology in resonance condition, $R_{L,opt}$ is given by:

$$R_L = R_2\sqrt{1+\frac{(\omega_0 M)^2}{R_2 R_1}} \quad (7)$$

For a given operational frequency, the maximum efficiency can be achieved by varying the coil configurations, i.e., R_1, R_2, M. The ferrite core provides a path of low reluctance for the magnetic flux, as shown in Fig. 5, which is denoted by C_{core}, L_{core} and R_{core}. The most difficult parameter to predict a priori is typically the loss in the magnetic core, namely R_{core}. The mutual inductance between L_1 and $L_2 + L_{core}$ is represented as M′ However, a drawback of using magnetic cores is that the magnetic core material introduces additional energy dissipation (loss) mechanisms, represented by R_{core}.

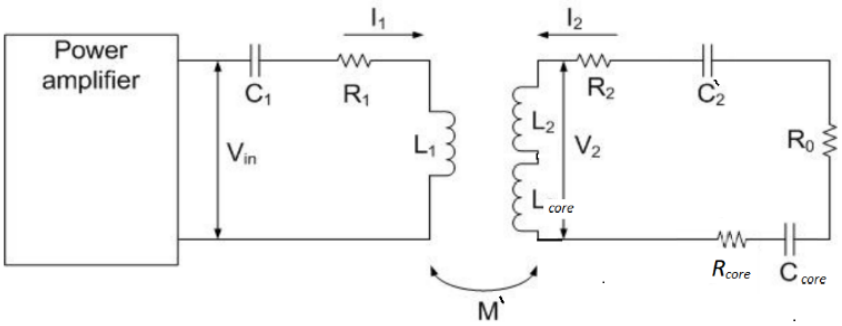

Fig. 5. Equivalent circuit of the system. Coils with a ferrite core.

According to Eq. (5), the transfer efficiency of the WPT system with the ferrite core η can be calculated:

$$\eta' = \frac{(\omega_0 M')^2 R_L}{(R_2+R_L+R_{core})(R_1(R_2+R_L+R_{core})+(\omega_0 M')^2)} \quad (8)$$

A magnetic core is a piece of magnetic material with a high magnetic permeability, high electrical resistivity, low coercive field strength, and low core loss used to confine and guide magnetic fields in electrical devices. By using a magnetic core, the magnetic field strength inside the coil can be increased. Lindberg and Kaikkonen gave the core loss formulation which is dependent complex permeability of core [22].

From an equivalent circuit perspective, the ferrite core increases the mutual coupling between a transmitter coil and receiver coil, M′, which is critical for achieving higher power transfer efficiency at longer distances. Furthermore, the total mutual inductance, M′ accounting for the ferrite effect can be written as [23-24]:

$$M' = M\ FF \quad (9)$$

where FF is the ferrite factor, effectively increasing observed coupling.

The effect of a ferromagnetic rod of radius r_{core}, l_{core} length and relative permeability μr is summarized as [25]:

$$FF = \left(1 - \left(\frac{r_{core}}{r_s}\right)^2\right) + \sqrt[3]{\frac{l_{core}}{l_s}} \frac{\mu_r}{1+D_{fe}(\mu_r-1)} \cdot \left(\frac{r_{core}}{r_s}\right)^2 \quad (10)$$

where l_s is the length of the secondary winding. The demagnetization factor D_{fe} calculates as [24]:

$$\begin{cases} D_{fe} = \frac{1.7(0.5\delta)^{0.13}}{\alpha^3}\left(\frac{1}{\delta}\right)^2\left(\ln\left(\frac{1+\alpha}{1-\alpha}\right) - 2\alpha\right), & \delta = \frac{l_{core}}{r_{core}} > 2 \\ D_{fe} = 0.33, & \delta = \frac{l_{core}}{r_{core}} = 2 \\ D_{fe} = \frac{3.966(0.5\delta)^{-0.056}}{\alpha^3}\left(\frac{1}{\delta}\right)^2(\alpha - \text{aran}(\alpha)), & \delta = \frac{l_{core}}{r_{core}} < 2 \end{cases} \quad (11)$$

The α parameter defines as:

$$\alpha = \sqrt{\left(1 - \left(\frac{2}{\delta}\right)^2\right)} \quad (12)$$

The continuously varying radius of the loop of a spiral coil is calculated by considering coils as an Archimedean spiral [23]. Accounting for the ferrite effect [24], L_2 is rewritten as;

$$L_{core} = L_2\, FF \quad (13)$$

The inductance calculation L is made using [8]:

$$L = \frac{N^2(D_0 - N(w+p))^2}{16D_0 + 28N(w+p)} \frac{39.37}{10^6} \quad (14)$$

where N is number of coil turns, D_0 is the outer diameter of the coil, w is the wire diameter, and the coil pitch p.

The presented solution is only an approximation of the actual core effect. Because of the magnetic flux leakage from rod ends, the flux density in a cylindrical core volume is not constant, as assumed during derivation of the above formulae in [14].

Alternate method supports calculation of core losses using a complex permeability characteristic identified for a given rod core design. Similarly, the equivalent resistance R_{core} is defined, yet aligned with a coil inductance L containing ferromagnetic core, as [18]:

$$R_{core} = \omega \frac{\mu''}{\mu'} L = \omega\, L\, tg(\gamma) \quad (15)$$

where γ is called magnetic loss tangent and μ′, μ″ result from the complex permeability μ of a ferromagnetic material defined as [22]:

$$\mu = \mu' - j\mu'' \quad (16)$$

To calculate the mutual inductance on the base of the method presented in [15], rectangular sections of primary and secondary coils are discretized into (2N+1)×(2S+1) and (2n+1)×(2m+1) subsections. Subsequently, the mutual inductance between each subsection of primary and secondary coils is calculated using Eq. (17), observing radial and axial change of coordinates. To apply the filamentary method to a solid conductor turn, the coil's cross-section is virtually divided into several smaller rectangular subsections, assuming the same current flowing through each filament. Such a discretization process is presented in Fig. 6. In practice, the number of discretization cells is limited by the required accuracy, which increase is not observed for a significantly extended resolution. For typical cases, it is enough to use up to 9-25 subdivisions [20-21], [25]. Within the last step, individual contributions are summed up, scaled by the number of discretization cells, and multiplied by the number of turns N_p, N_s. The below formula explains this process [14-15]:

$$M = \frac{N_p N_s \sum_{g=-K}^{g=K} \sum_{h=-N}^{h=N} \sum_{p=-m}^{p=m} \sum_{l=-n}^{l=n} M(g,h,p,l)}{(2K+1)(2N+1)(2m+1)(2n+1)} \quad (17)$$

The exact form of parameters used by the nominator of Eq. (17) is presented in [15].

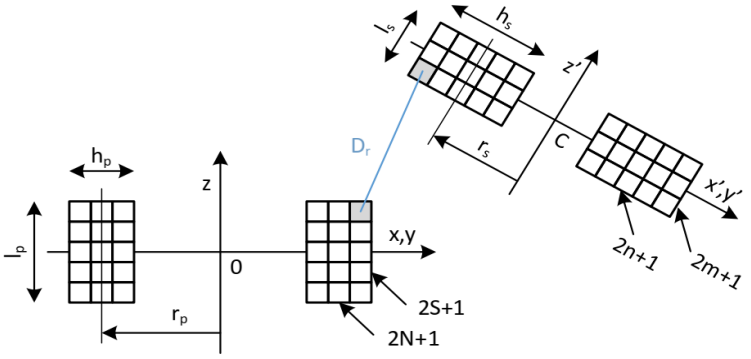

Fig. 6. Discretization of coil sections [15].

3. RESULTS AND DISCUSSION

A 1.5 mm-diameter, 10 mm-length 3C90 ferrite rod from Fair-Rite Products, Corp., Wallkill, NY, US, with a relative permeability μr of 2300 is chosen as core for the tiny-coil and 490 turns are manually wound around the rod in a single layer. Fig. 2 illustrates the intended arrangement of the external (primary) coil and the implanted (secondary) coils, for the proposed application of this work. The estimation of core loss using complex relative permeability data of 3C90 material, together with core effect, results in R_{core} = 0.095 Ω for 125 kHz assuming L= 1.64 mH. This loss increases up to R_{core} = 29.24 Ω for 1 MHz. The secondary coil used N_s = 490, h_s = 0.4 mm, l_s = 8.8 mm, and r_s= 0.95 mm. The primary coil, reflecting notation from Fig. 2, was arranged with N_p= 94, h_p= 1.2 mm, l_p = 2.8 mm, and r_p = 26.1 mm. The receiver coil would be a much smaller solenoid, approximately 1.5 mm in diameter, and would always be positioned inside the primary coil.

The number of subdivisions used in Eq. (17) was set as 15, thus N = S= m = n = 15. Two movement cases of the secondary coil were evaluated: the axial displacement within 0…..100 mm range and the lateral displacement 0 ….100 mm, with the radius r_p, as clarified in Fig. 3. As described in section 1, beginning at the horizontal and vertical centre of the primary, the ferrite volume was moved radially outward to 0 mm and 100 mm, and vertically upward to 0 mm and 100 mm.

Figs. 7 and 8 shows the calculated mutual inductance of the RX coils without the ferrite rods are lower compared to the RX coils with ferrite rods. The goal of this work is to determine the accuracy of Eq. (10) in most practical displacements of the coils. To achieve this, two independent configurations are realized; on the base of coils without cores and utilizing a core surrounded in a secondary coil.

The core increases the magnetic coupling, making WPT more efficient. Inserting a ferrite rod within the RX coil can amplify the flux density B through the coils volume and thus increase M. When ferromagnetic material is inserted within the coils, increases due to an increase in permeability and thus an enhancement of the magnetic flux through the coil's volume [7]. Therefore, it should be pointed out that the effect of mutual inductance is reduced at a longer transfer distance, and there are other factors affecting the transfer performance of the WPT system. This performance enhancement, which can overcome losses due to size decreases in the RX coil, is highly dependent on the shape and material properties of the ferrite. For this core data, the ferrite factor calculated according to Eq. (10) is FF= 18.24 ± 0.05. Good agreement is observed between the calculated, simulated and measured results. As shown in the air gap

analysis in Fig. 7 and Fig. 8, it is seen that the lowest mutual inductance value is obtained in the shielded-coreless condition. From Figures, it can be observed that the shape of the curves from the simulations and measurements shows similar behavior.

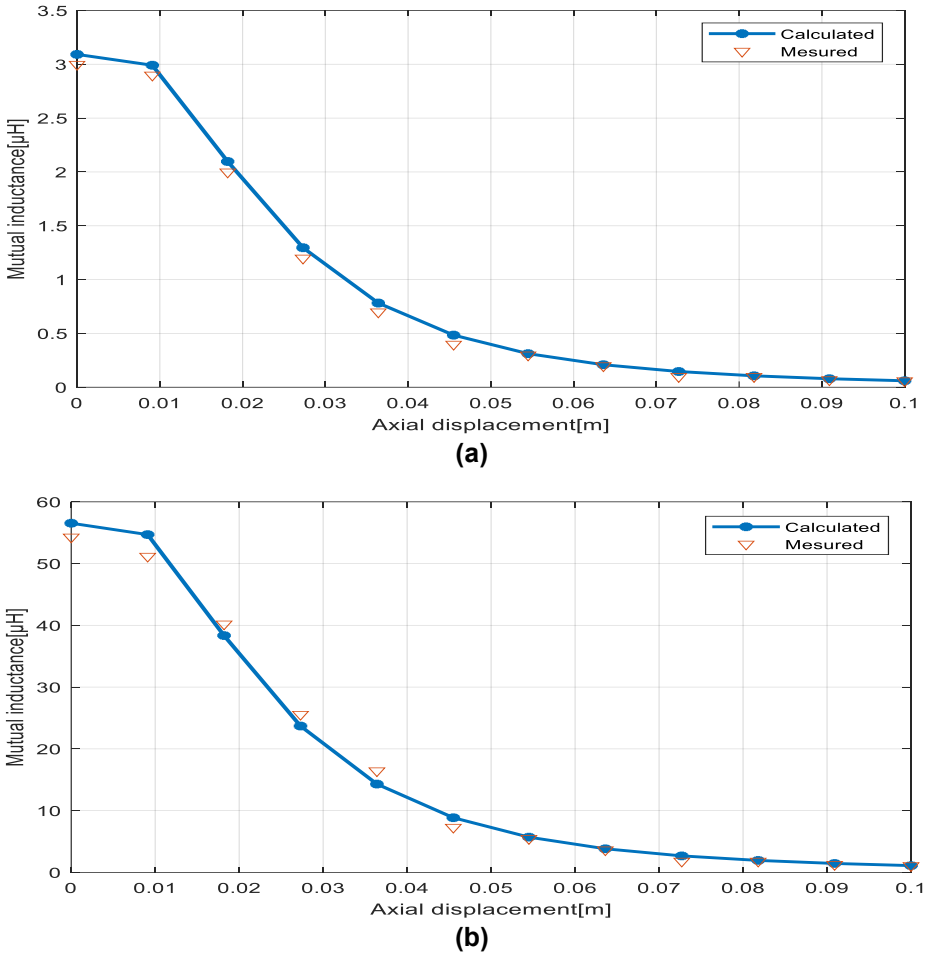

Fig. 7. Comparison of calculated, simulated and measured data for axial displacement of the secondary coil: a) without the ferromagnetic core; b) with the ferromagnetic core.

Fig. 9 shows the load power and efficiency while keeping the receiver centered, but moving it away from the transmitter to a maximum height of 100 mm. Here a 500 Ω load resistance was used with the receiver. The simulated output power is shown as a function of axial displacement in Fig. 9. At c = 26 mm, the power received is 14 W, which corresponds to a power transfer efficiency of 60 %. Nevertheless, the receiver was still able to draw a power of 6 W at 89% efficiency at a height of 10 mm, and 6 W at 13% efficiency at 50 mm. From Fig. 9 it can be deduced that with an increase in axial displacement, the practically calculated PTE values decrease, as can be predicted from the theoretical equations. It is worth mentioning that PTE and PL are highly dependent on the relative distance between the TX/RX pairs.

Receiver performance was also evaluated as a function of lateral distance from the center of the transmitter with the receiver in contact with the transmitter. The WPT prototype is calculated for a load of 500 Ω and a distance between the primary and the secondary of 26 mm corresponding to our target study case. This result is plotted in Fig. 10, where it is seen that the PTE and PL begins at approximately 57 % and 14 W and then rises up to a value of 1 % and 1 W at d=40 mm before eventually reaching zeros in the far distance.

Fig. 9 and Fig. 10 shows the use of the ferrite-core receiver facilitates relatively broad lateral freedom, allowing high power and efficiency, so long as the receiver is positioned within

the extents of the transmitter windings. Systems such as biomedical implants may be able to take advantage of these lateral degrees of freedoms.

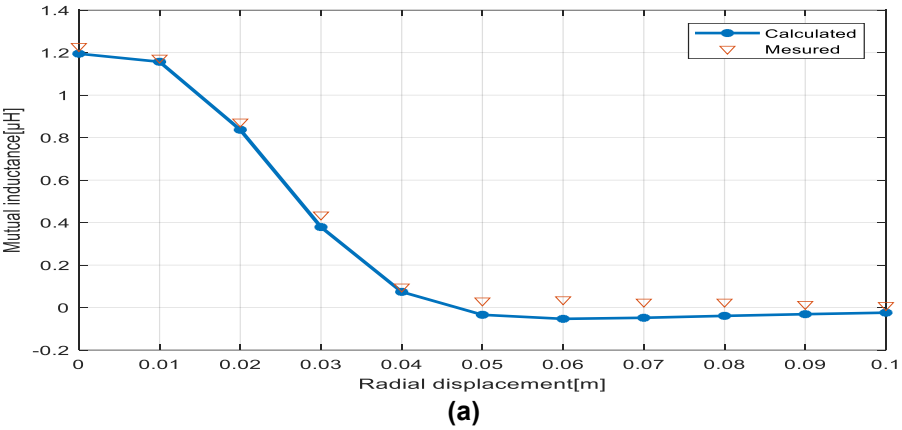

Fig. 8. Comparison of calculated and measured data for a radial displacement of the secondary coil : a) without the ferromagnetic core; b) with the ferromagnetic core.

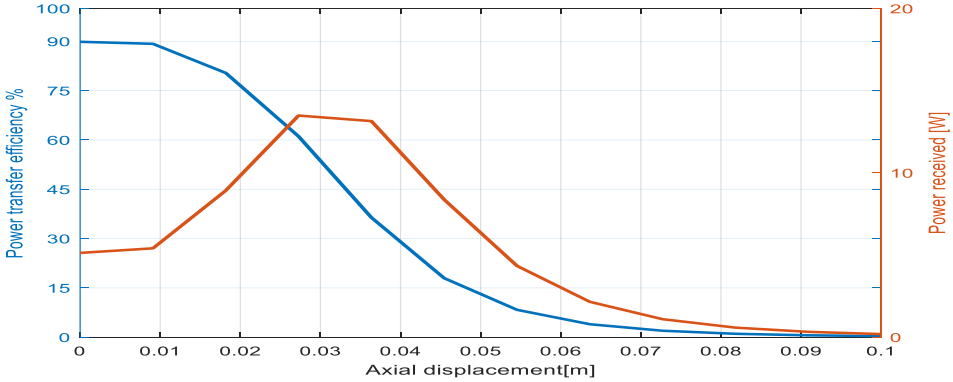

Fig. 9. Output power and system efficiency at different heights above the transmitter.

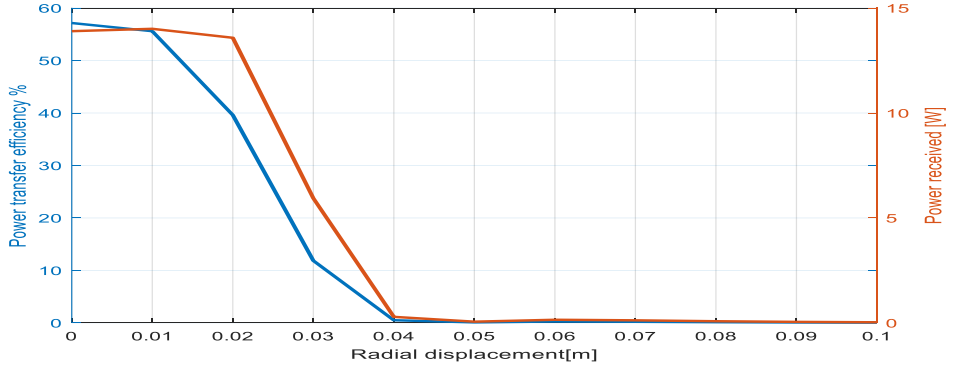

Fig. 10. Output power and system efficiency at different lateral offset locations.

The power transfer efficiency and power received at two operation frequencies have also been calculated, as plotted in Figs. 11 and 12. The power transfer efficiencies at 0.5 MHz and 1 MHz are given in these Figures, as functions of the separation distance between the coil pairs.

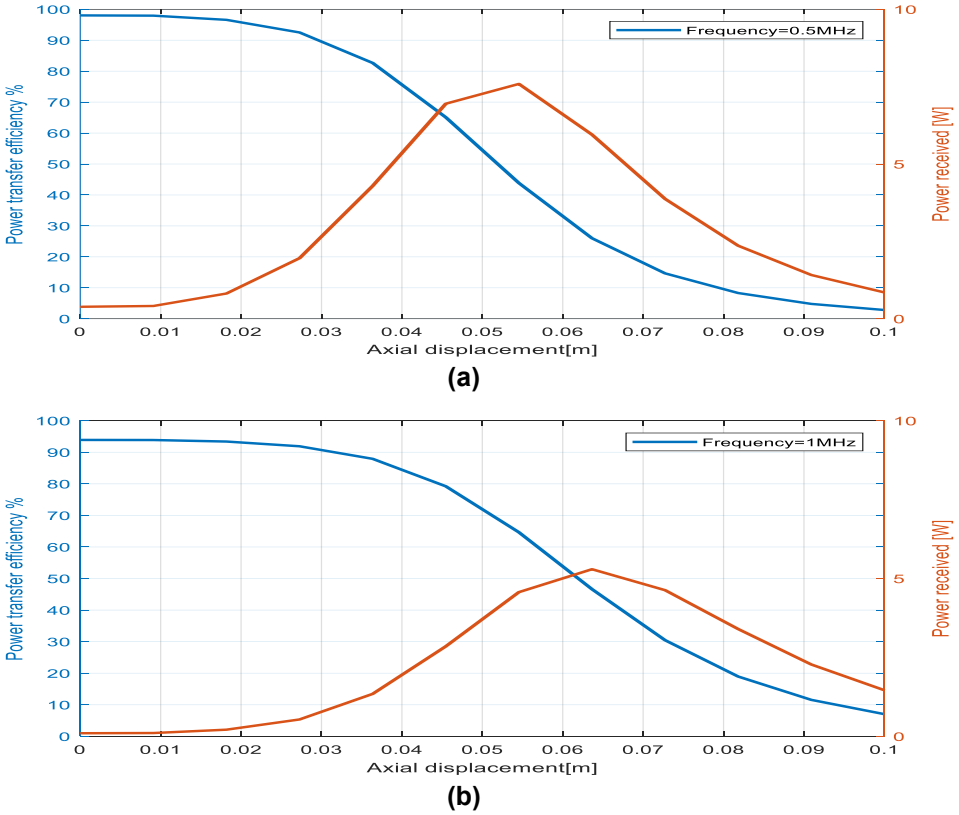

Fig. 11. Output power and system efficiency at different axial offset locations: a) f=0.5 MHz, b) f=1 MHz.

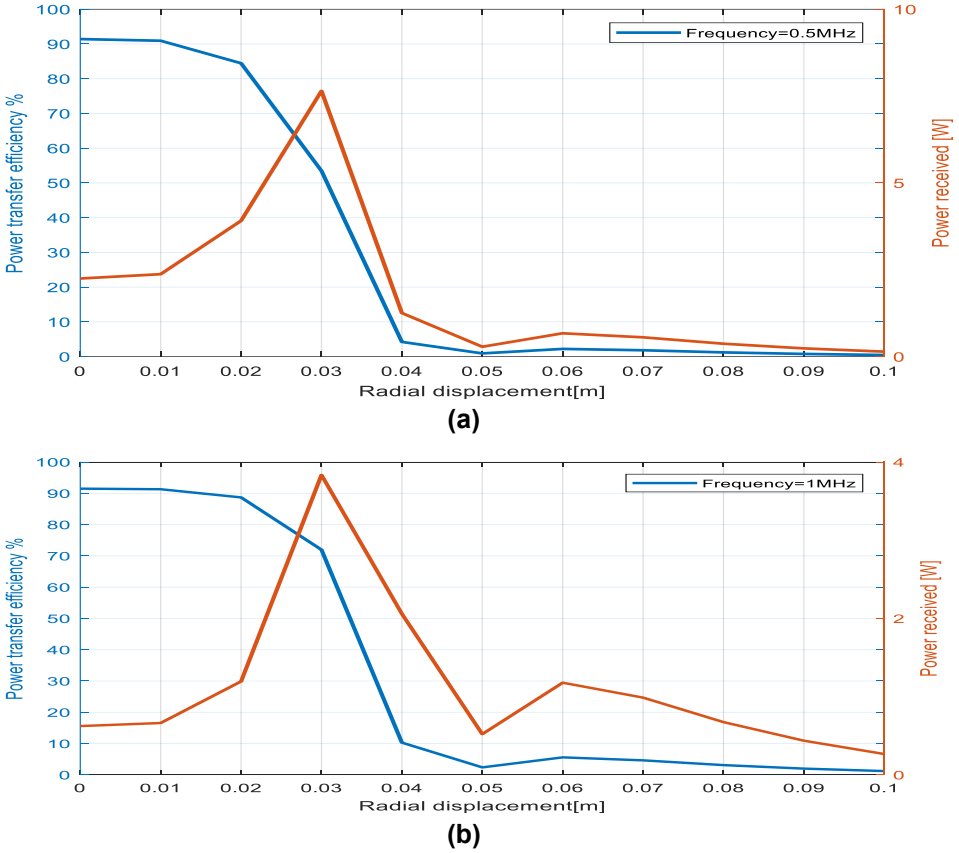

Fig. 12. Output power and system efficiency at different lateral offset locations: a) f=0.5 MHz, b) f=1 MHz.

The results show that the power received is diminished by more than two times as the operation frequency is changed from 0.5 MHz to 1 MHz. Overall, the power transfer efficiencies are low and drop quickly as the separation distance increases. However, when the two coils are misaligned, the magnetic fields no longer interact optimally, decreasing power transfer efficiency. The power transfer efficiency is below 2 % at the radial distance of 50 mm (Fig. 12), indicating more power will be required on the primary stage in order to obtain enough power for the RX coil. The most effective way to enhance the power received is to decrease the frequency. The results clearly show that the frequency 0.125 MHz is the best in terms of both efficiency and transferred power (Fig. 9).

The results demonstrate that with a frequency of 0.5 MHz, the WPT system has a higher output power and efficiency than the frequency 1MHz. Under the same conditions of output power and transmission efficiency, the WPT system has a greater transmission distance when the d=30 mm. Therefore, it can be concluded that the lower operating frequency limit produces higher PTE values whereas the higher operating frequency limit produces higher P_L values.

Higher frequencies are associated with smaller coils, which is advantageous in this case. However, with increasing frequency, the losses in the coil also increase [23]. In practice, the WPT frequency of inductive links like the one under consideration, designed for the transfer of tens to hundreds of mW over a distance smaller than the coil radius, is therefore often chosen below 30 MHz. Considering the above, we have chosen to operate the WPT link for this work at 0.125 MHz.

To determine the maximum power that the receiver could harvest from the transmitter, a range of load resistances were tested to determine the ideal load resistance. We studied the simulated performance of the RX coil versus load resistance. In order to investigate the influence of the load on the WPT performances, the analysis of the efficiency is carried out by varying R_L in the range 0-50 Ω.The obtained results are shown in Fig. 13, highlighting as this WPT system can operate very well for a wide range of R_L values. As shown in Fig. 13, the load resistance does have a significant effect on the power transfer efficiency and power received. The efficiency is very important parameter for power transfer systems and as shown in Fig. 13, the efficiency increased with the increment in RL. However, the disadvantage is decreasing the power received PL.

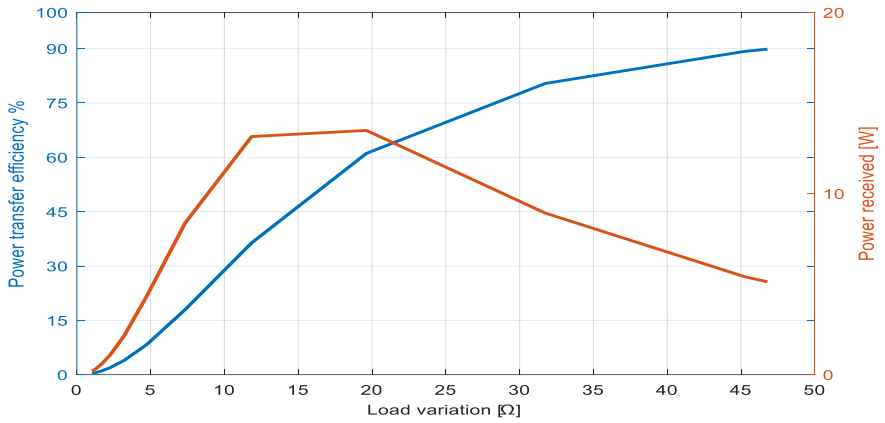

Fig. 13. Output power and system efficiency versus load resistance.

We noticed that the maximum value of P_L occurs at the 20 Ω, whereas at 47 Ω has lower transfer coefficient and smaller received power. It can be noted that the load resistance has a small effect on the values of and P_L for coil in the range of R_L = [18 Ω to 25 Ω]. They reach their

maximum of P_L and PTE = 62 % at R_L=20 Ω , then these values drop rapidly after R_L increases to more than P_L=5 W. It can be seen from Fig. 13, the output power PL is smaller when R_L is larger, so R_L is getting smaller to decrease the input power. This is in contrast to the performance obtained in relation to the power output. It is noted that an increase in load resistance leads to a corresponding decrease in power output. For example, the RX coil achieved a maximum efficiency of 90 % at a load resistance of 47 Ω with an output power of 5 W while maximum power of 14 W was transferred at a load resistance of 20 Ω at an efficiency of 61 %. For practical design implementation, there is always a trade-off between power output and efficiencies depending on the critical requirements for the system operations.

Due to this inverse relationship, the selection of the appropriate load resistance is dependent on the type of application. If the system design is aimed at high power transferred, increasing the load resistance is the most viable option. Thus, for the proposed coil designs employing the SS compensation topology, a load resistance of 20 Ω was selected as the optimum load resistance.

4. CONCLUSION

This work presents practical methods for determining the magnetic coupling between coils, expressed by the mutual inductance and the coupling factor. In particular, the results of the analytical solution is verified by measured mutual inductance of the configuration consisting of the air and ferromagnetic core coils. Firstly, the analytical methods used for calculating the mutual inductance were presented, indicating the possibility of using the filamentary method to analyze the complex, multilayered coil structures in a low-frequency band. Secondly, the effect of the presence of the ferromagnetic core inside a coil was reviewed. It was highlighted that mutual inductance would change due to the core material and core dimensions, although existing rod anisotropy may influence the overall accuracy of the analytical solution. In particular, the comparison of the solutions based on the calculation and measurement were analyzed. In general, the measured values seem to be consistent with the simulated ones.

In this paper, a folded cylindrical helix resonator is utilized to obtain the efficiency of 57% with the frequency of 0.125 MHz when the distance is 40 mm. we see that both the Output power and system efficiency is decreasing with transmission distance. As expected from the calculations, the efficiency had its peak at 26 mm for the simulated result. Nevertheless, there is a great demand of power conversion, and it is only suitable in low power applications. Consequently, the proposed system is a potential candidate for an alternative power source in capsule endoscopy.

This research introduces a computationally efficient analytical model for WPT in deep implants, bridging the gap between theoretical electromagnetics and practical biomedical engineering. By validating the model against experimental measurements of multi-axial displacements and accounting for the Fill Factor of laminated cores, this work provides a transparent alternative to FEM for optimizing the safety and efficiency of miniaturized medical devices.

REFERENCE

[1] Z. Zhang, H. Pang, A. Georgiadis, C. Cecati, "Wireless power transfer-An overview," *IEEE Transactions on Industry Electronics*, vol. 66, pp.1044–1058, 2019, doi:10.1109/TIE.2018.2835378.

[2] J. Zhiwei, Y. Guozheng, W. Zhiwu, L. Hua, "Efficiency optimization of wireless power transmission systems for active capsule endoscopes," *Physiological Measurement*, vol. 32, no. 10, pp. 1561–1573, 2011, doi:10.1088/0967-3334/32/10/005.
[3] A. Ibrahim, M. Kiani, "A figure-of-merit for design and optimization of inductive power transmission links for millimeter-sized biomedical implants," *IEEE Transactions on Biomedical Circuits and Systems*, vol. 10, pp.1100-1111, 2016, doi:10.1109/TBCAS.2016.2515541.
[4] P. Wang, Y. Sun, Z. Liao," An optimal design method of coils for magnetic coupled wireless power transfer system," Proceeding of the Progress in Electromagnetics Research Symposium, 2018.
[5] D. Ahn, M. Ghovanloo, "Optimal design of wireless power transmission links for millimeter-sized biomedical implants," *IEEE Transactions on Biomedical Circuits and Systems*, vol. 10, pp. 125–137, 2016, doi: 10.3390/electronics9122130.
[6] P. Theilmann, P. Asbeck, "An analytical model for inductively coupled implantable biomedical devices with ferrite rods," *IEEE Transactions on Biomedical Circuits and Systems*, vol. 3, no. 1, pp. 43-52, 2009, doi: 10.1109/TBCAS.2008.2004776.
[7] P. Feng, P. Yeon, Y. Cheng, M. Ghovanloo, T. Constandinou,"Chip-scale coils for millimeter-sized bio-implants," *IEEE Transactions on Biomedical Circuits and Systems*, vol. 12, no. 5, pp. 1088–1099, 2018, doi: 10.1109/TBCAS.2018.2853670.
[8] Y. Jia et al., "Position and orientation insensitive wireless power transmission for enerCage-homecage system," *IEEE Transactions on Biomedical Engineering*, vol. 64, no. 10, pp. 2439–2449, 2017, doi:10.1109/TBME.2017.2691720.
[9] A. Amezani, S. Farhangi, H. Iman-Eini, B. Farhangi, R. Rahimi, G. Moradi, "Optimized lCC-series compensated resonant network for stationary wireless chargers," *IEEE Transactions on Industrial Electronics*, vol. 66, pp.2756–2765, 2019, doi: 10.1109/TIE.2018.2840502.
[10] K. Song, Z. Li, J. Jiang, C. Zhu,"Constant current/voltage charging operation for series-series and series-parallel compensated wireless power transfer systems employing primary-side controller," *IEEE Transactions on Power Electronics*, vol. 33, pp. 8065–8080, 2017, doi: 10.1109/TPEL.2017.2767099.
[11] N. Mohdeb," Comparative study of circular flat spiral coils structure effect on magnetic resonance wireless power transfer performance," *Progress In Electromagnetics Research M*, vol. 94, pp.119-129, 2020, doi:10.2528/PIERM20051705.
[12] S. Babic, F. Sirois, C. Akyel, C. Girardi, "Mutual inductance calculation between circular filaments arbitrarily positioned in space: Alternative to Grover's Formula," *IEEE Transactions on Magnetics*, vol. 46, pp. 3591-3600, 2010, doi:10.1109/TMAG.2010.2047651.
[13] M. Basar, M. Ahmad, J. Cho, F. Ibrahim, "A wireless power transmission system for robotic capsule endoscopy: Design and optimization," IEEE MTT-S International Microwave Symposium Digest, 2014, doi: 10.1109/MWSYM.2014.6848451.
[14] Z, Zheng, X. Fang, "A wireless power transfer system based on dual-band metamaterials,'' *IEEE Microwave and Wireless Technology Letters,* vol. 32, pp. 615-618, 2022, doi: 10.1109/LMWC.2022.3140535.
[15] J. Zhang et al., "A high-efficiency wireless power transfer system with flexible receiver coil for capsule endoscopy," *IEEE Transactions on Biomedical Circuits and Systems*, vol. 15, no. 1, pp. 46–56, 2021, doi:10.1109/TBCAS.2021.3053495
[16] J. Wang, M. Leach, E. Lim, Z. Wang, R. Pei, Y. Huang, "An implantable and conformal antenna for wireless capsule endoscopy," *IEEE Antennas and Wireless Propagation Letters*, vol. 17, no. 7, pp. 1153–1157, 2018, doi: 10.1109/LAWP.2018.2836392.
[17] X. Liu et al., "A Misalignment-tolerant wireless power transfer system for medical implants using a Hemispherical Transmitter," *IEEE Transactions on Power Electron*, vol. 38, no. 4, pp. 5521–5534, 2024, doi: 10.1109/TPEL.2024.3353521.
[18] A. Essa, E.Almajali, S. Mahmoud, R. Amaya, S. Alja'Afreh, "Wireless power transfer for implantable medical devices: impact of implantable antennas on energy harvesting", *IEEE Open Journal of Antennas and Propagation*, vol. 5, no.3, pp. 739-758, 2024, doi:10.1109/OJAP.2024.3396541.
[19] P. Guan, Y. Ren, C. Tang, L. Wang, B. Luo, Y. Lin, "Electromagnetic analysis and experimental study of laminated Mn-Zn toroidal ferrite cores for high-frequency inductance and impedance enhancement", *Micromachines*, vol. 43, p. 17, 2026, doi: 10.3390/mi17010043.
[20] X. Wei, Z. Wang, H. Dai, "A critical review of wireless power transfer via strongly coupled magnetic resonances", *Energies*, pp. 4316-4341, 2014, doi:10.3390/en7074316.

[21] D. Kim, Y. Park, "Calculation of the inductance and AC resistance of planar rectangular coils," *Electronics Letters*, vol. 52, no. 15, pp.1321-1323, 2016, doi:10.1049/el.2016.0696.
[22] Q. Wang, W. Che, M. Dionigi, F. Mastri, M. Mongiardo, G. Monti," Gains maximization via impedance matching networks for wireless power transfer", *Progress In Electromagnetics Research*, vol. 164, pp. 135-153, 2019, doi:10.2528/PIER18102402.
[23] K. Tec, I. Takehir, O. Sehoo, H. Yoich, "Automated impedance matching system for robust wireless power transfer via magnetic resonance coupling", *IEEE Transactions on Industrial Electronics*, vol. 6, pp-3689-3698, 2013, doi:10.1109/TIE.2012.2206337.
[24] L. Che, S. Liu, Y. Zho, T. Cui, "An optimizable circuit structure for high-efficiency wireless power transfer", IEEE Trans. Industrial Electronics, vol. 6, pp. 339-349, 2013, doi: 10.1109/TIE.2011.2179275.
[25] D. Mukherjee, S. Kaur, R. Singh, D. Mallickn", "A miniaturized, low-frequency magnetoelectric wireless power transfer system for powering biomedical implants", *IEEE Transactions on Biomedical Circuits and Systems*, vol. 18, no. 3, pp. 438-450, 2024, doi: 10.1109/TBCAS.2023.3336598.